

1 **Optimum performance investigation of LYSO**
2 **crystal pixels: A comparison between GATE**
3 **simulation and experimental data**

4 **Ze Chen**

5 Institute of Modern Physics, Chinese Academy of Sciences, Lanzhou 730000, China
6 University of Chinese Academy of Sciences, Beijing 100049, China

7 E-mail: chenze@impcas.ac.cn

8 **Zheng Guo Hu**

9 Institute of Modern Physics, Chinese Academy of Sciences, Lanzhou 730000, China

10 E-mail: huzg@impcas.ac.cn

11 **Jin Da Chen**

12 Institute of Modern Physics, Chinese Academy of Sciences, Lanzhou 730000, China

13 E-mail: chenjinda@impcas.ac.cn

14 **Xiu Ling Zhang**

15 Institute of Modern Physics, Chinese Academy of Sciences, Lanzhou 730000, China

16 E-mail: xiuling@impcas.ac.cn

17 **Zhi Yu Sun**

18 Institute of Modern Physics, Chinese Academy of Sciences, Lanzhou 730000, China

19 E-mail: sunzhy@impcas.ac.cn

20 **Wen Xue Huang**

21 Institute of Modern Physics, Chinese Academy of Sciences, Lanzhou 730000, China

22 E-mail: huangwx@impcas.ac.cn

23 **Jian Song Wang**

24 Institute of Modern Physics, Chinese Academy of Sciences, Lanzhou 730000, China

25 E-mail: jswang@impcas.ac.cn

26 **Zhong Yan Guo**

27 Institute of Modern Physics, Chinese Academy of Sciences, Lanzhou 730000, China

28 E-mail: guozhy@impcas.ac.cn

29 **Guo Qing Xiao**

30 Institute of Modern Physics, Chinese Academy of Sciences, Lanzhou 730000, China

31 E-mail: xiaogq@impcas.ac.cn

32 **Abstract.** Monte Carlo simulation plays an important role in the study of time of
33 flight (TOF) positron emission tomography (PET) prototype. As it can incorporate
34 accurate physical modeling of scintillation detection process, from scintillation light
35 generation, the transport of scintillation photons through the crystal(s), to the
36 conversion of these photons into electronic signals. The Geant4 based simulation
37 software GATE can provide a user-friendly simulation platform containing the
38 properties needed. In this work, we developed a dedicated module in GATE simulation
39 tool. Using this module, we simulated the light yield, energy resolution, time resolution
40 of LYSO pixels with the same cross-section ($4 \times 4 \text{ mm}^2$) of different lengths: 5 mm, 10
41 mm, 15 mm, 20 mm, 25 mm, coupled to a PMT. The experiments were performed to
42 validate the GATE simulation results. The results indicate that the best time resolution
43 ($484.0 \pm 67.5 \text{ ps}$) and energy resolution ($13.3 \pm 0.4 \%$) could be produced by using pixel
44 with length of 5 mm. The module can also be applied to other cases for precisely
45 simulating optical photons propagating in scintillators.

46 1. Introduction

47 In the development of time of flight (TOF) positron emission tomography (PET)
48 detectors, understanding and optimizing scintillator light collection, energy resolution
49 and time resolution is critical for achieving high performance. Monte Carlo simulations
50 play an important role in guiding research in detector designs, as it can vary many design
51 parameters much more easily. The Geant4 [1] based simulation platform GATE [2],
52 which provides a user-friendly, scripted interface, has come into widespread use in the
53 field of nuclear medicine for simulating PET devices.

54 The widely used LYSO:Ce crystal has high density ($7.40 \text{ g}\cdot\text{cm}^{-3}$), high light
55 output (26,000 photons/MeV), good energy resolution (15%) and short decay time (40
56 ns) [3], [4], which makes it a good candidate in the study of TOF-PET prototype. We
57 adapted crystal array which consisted of the LYSO crystal pixels to improve the spatial
58 resolution of our detector modules. From the very beginning, we would like to know the
59 performance of LYSO pixels.

60 The objective of the work is to validate the reliability of the dedicated module used
61 in GATE simulation tool and compare the predicted light yield, energy resolution and
62 time resolution with experimental results.

63 2. Simulation Model and Method

64 The detector is contained within a world volume, which consists of LYSO crystal
65 coupled to photomultiplier tube (PMT), which is shown in Fig.1. Some elementary

66 properties of the different materials used in the simulation are given in table 1. Three-
 67 part physics process are involved in the simulation: γ -ray interaction in detector; the
 68 scintillation light emission and light transport inside the detector and the photoelectron
 69 generation; anode signal generation in the PMT and electron process which involves the
 70 time discriminator.

71 *2.1. γ -ray Generation and Interaction in Detector*

72 In GATE simulation, 511 KeV γ -rays imping laterally on different length LYSO crystal
 73 pixels at the smallest cross-section ($4 \times 4\text{mm}^2$). In the process of simulation, we change
 74 nothing but the length of the LYSO pixel from 5 mm to 25 mm by a step of 5 mm.

75 *2.2. Scintillation light emission and transport*

76 The scintillation light emission in GATE was described by the total light yield, rise time,
 77 decay time, resolution scale, and bulk light attenuation length, which are listed in table 2.

78 The light transport process in the detector is very complicated. We use the
 79 UNIFIED model [5] to model the reflection of the photons at surfaces between two
 80 dielectric materials. In this study, we use ground and ground-back-painted. A ground
 81 surface is assumed to consist of small micro-facets, whose normals have small angles
 82 relative to the average surface normal. The distribution of these angles is assumed to be
 83 Gaussian with mean 0 and standard deviation σ_α . The type and surface finish of each
 84 of the optical interfaces defined in the simulations have been given in table 3.

85 *2.3. PMT response*

86 The PMT response of single photoelectron is a current signal that can be described as
 87 a Gaussian pulse [6]:

$$88 \quad i_{pe}(t) = \frac{G}{\sqrt{2\pi}\sigma} \exp\left(-\frac{t^2}{2\sigma^2}\right) \quad (1)$$

89 G = Parameter related to the gain of PMT,

90 σ = Time constant that determines the width of the pulse.

91 The anode output circuit can be considered as a parallel of a load resistor (R_L) and
 92 parasitic capacitor (C). The impulse response of the circuit is:

$$93 \quad h(t) = \frac{1}{C} \exp\left(-\frac{t}{\tau}\right) \quad (2)$$

94 $\tau = R_L C$

95 The single photoelectron anode response (v_{pe}) was the convolution of the anode
 96 current and the output circuit [7]:

$$97 \quad v_{pe}(t) = \frac{G}{\sqrt{2\pi}\sigma C} \cdot \int_0^t \exp\left(-\frac{t-x}{\tau}\right) \cdot \exp\left(-\frac{t^2}{2\sigma^2}\right) dx \quad (3)$$

98 The PMT output signal was the sum of the anode pulses of all the photoelectrons:

$$99 \quad V(t) = \sum_{i=1}^{N_{pe}} v_{pe,i}(t - t_{pe,i}) \quad (4)$$

100 Fig. 5 shows a simulated LYSO pixel signal of a 511 keV γ -ray event. The data
101 includes the photoelectrons time distribution on the photocathode, the PMT output
102 signal of a gamma event and the normalized PMT response of single photoelectron(pe),
103 Here normalized means that the photoelectron distribution is divided by the height of
104 the spectrum.

105 3. Experimental studies

106 3.1. Set up

107 The LYSO pixels with various lengths and same cross-section($4 \times 4mm^2$) are used in the
108 experiment, which are illustrated in Fig. 2. Since the naturally radioaction of Lu(176)
109 in LYSO, a coincidence detection circuit was adapted in order to eliminate the LYSO
110 background. The collimator is 8 cm thick lead block with 4 mm diameter holes, which
111 is set on a position system able to move along both the x- and y-axis. A plane ^{22}Na
112 source was placed in the center of the lead block. The coincidence detector module
113 consists of a $\phi 3$ cm LaBr₃ crystal, which is produced by Saint-Gobain, coupled to a
114 Hamamatsu R4998 PMT, biased by a high-voltage power supply ORTEC Model 556
115 with a negative voltage of 1400V. The imaging detector module consists of a LYSO pixel
116 which is produced by Sinoceramics, Inc., coupled to a Photonics XP20D0 PMT, biased
117 by the same high-voltage power supply with a negative voltage of 1000 V. The LaBr₃
118 detector and the imaging detector were placed on two position systems respectively,
119 which could move along both the x- and z-axis. By moving the LaBr₃ detector, imaging
120 detector and lead collimator, the collimated 511keV flux could reach both faces of
121 two detector modules. To increase the collection efficiency for light photons produced
122 by absorption of γ -rays, the samples under investigation were coated with Enhanced
123 Spectular Reflector(ESR). Optical contact between the scintillation crystal and PMT
124 photocathode is maintained by an optical grease.

125 3.2. Coincidence acquisition system

126 The coincidence acquisition system and signal flow is illustrated in Fig. 3. Both the
127 imaging and coincidence detector modules processing units are identical. The dynode
128 signals were transmitted to the coincidence module(Ortec CO4020) via a time filter
129 amplifier(TFA, Ortec 474), a constant fraction discriminator(CFD, Ortec CF8000) and
130 a delay(Ortec GG8000). The discriminated signals from CFD were also fed into TDC
131 module(Philips 7187). The anode signal flows were sent to an amplifier(Ortec 572) via a
132 preamplifier. The amplified signals were fed into ADC module(Philips 7164).

133 4. Comparison between simulation and experiment

134 4.1. Energy spectrum

135 Fig. 6 shows the energy spectra of LYSO pixels with different length. All spectrums are
136 normalized such that the full-energy peaks have equal heights. Both compton platform
137 and photo peak are well described by the GATE simulation with different pixel lengths.
138 The low energy part of measured spectrum was truncated due to the CFD setting. Slight
139 discrepancies between the experimental and simulated energy photopeak is observed but
140 these difference are not significant.

141 4.2. Light yield

142 For quantitative analysis, the simulated light output was derived by integrating the total
143 area under the histogram of photoelectrons from time zero to a time point which was
144 three times the decay constant of scintillation decay (Fig. 5(a)). The measured absolute
145 light yield of the scintillation pixel under investigation is determined by comparing the
146 postion of the full energy peak in the ^{22}Na spectra (511 keV) to the position of center-
147 of-gravity of the single-photoelectron spectrum [8], which is shown in Fig. 4. We use
148 multi-gaussian fit to the spectrum to find mean value of the single photo-electron peak,
149 which can be regarded as centr-of-gravity.

150 Fig. 7 shows absolute light yield as a function of the crystal length. The error bars
151 represent one standand deviation of uncertainty. A exponential fit was used to obtain
152 the attenuation length. The simulated effective attenuation length is 26.72 ± 0.06 mm,
153 less than the bulk length used above. The experimental attenuation is found to be equal
154 to 27.05 ± 0.06 mm. Good agreement is found between the simulation and experiment.

155 4.3. Energy resolution

156 For each energy spectrum, the energy resolution was obtained from a gaussian fit to
157 the photopeak. Fig. 8 shows the measured and simulated energy resolution of LYSO
158 pixels with different lengths. The error bars did not comprise systematics errors, but
159 only the statistical errors, which can be calculated from statistical uncertainties of the
160 fitted mean and sigma using propagation of errors formula. The larger error bar in pixel
161 of length 05 mm reflects the fact, shorter pixel has low-efficiency to detect γ -ray.

162 Modeled and measured energy resolutiion values agreed very well with discrepancies
163 limited to the range of -1.18 % to +1.12 % and an average absolute difference of 0.83 %.
164 This excellent agreement indicates that the energy resolutions observed in pixels with
165 different lengths can be reproduced and attributed entirely to statistical uncertainties
166 in the number of photoelectrons detected at the photocathode.

167 The tail pile-up is observed in Fig. 6(c). This may at least partially be caused
168 by the undershoots from preceding pulse during acquisition. In Fig. 6(e), a long tail
169 in high energy part of experiment spectrum is obvious, when compared to simulation
170 one. We find the similar tail in simulation by using a shorter bulk length (i.e. 30 mm)

171 in crystal setting. From this point of view, the effective attenuation length in pixel of
172 length 25 mm should be less than 26.5 mm, which may be caused by non-uniformity of
173 lyso pixel.

174 4.4. Time resolution

175 For both simulation and experiment, we use constant fraction discrimination (CFD) as
176 the time pick-off method. In the CFD implementation of the module, the original pulse
177 histogram is attenuated by a factor and then added to an inverted version of the raw
178 signal histogram with a delay. The time information can be derived by finding the
179 position of zero-crossing using interpolation. We can extract the time resolution Δt_s
180 from a gaussian fit to time information histogram. Since PMT transit-time-dispersion
181 (TTS) is independent of the scintillation and photo-electron conversion, so the detector
182 time resolution Δt_{det} is calculated with TTS (200 ps [9]) and Δt_s as [10]

$$183 \quad \Delta t_{det} = \sqrt{(\Delta t_s)^2 + (TTS)^2}. \quad (5)$$

184 Fig. 9 shows the time resolution obtained by simulation and experiment. The error
185 bars only comprise the statistical errors. Good agreement is found within the simulation
186 and experiment errors.

187 5. Conclusions and future work

188 We have developed a specified module in GATE simulation software, which has proved
189 to be reliable in fully simulating the optical photon processes in the pixel geometry.
190 This module can also easily be used for block geometry, which is consist with matrix of
191 pixels.

192 For future work, we will incorporate some mathematical models to accelerate
193 simulation process and simulate the optical processes in the Anger-logic based detector
194 to generate the spatial distribution information, from which light sharing can be
195 investigated.

196 Acknowledgements

197 This work is supported by National Natural Science Foundation of China
198 (11205222), West Light Foundation of the Chinese Academy of Sciences (210340XBO)
199 National Major Scientific Instruments and Equipment Development Projects
200 (2011YQ12009604) Youth Innovation Promotion Association, CAS201330YQO

201 References

- 202 [1] Agostinelli S *et al.* 2003 *Nucl. Instr. and Meth. A* **506** 250 – 303
203 [2] van der Laan D J J, Schaart D R, Maas M C, Beekman F J, Bruyndonckx P and van Eijk C W E
204 2010 *Phys. Med. Biol.* **55** 1659

- 205 [3] Korzhik M, Fedorov A, Annenkov A, Borissevitch A, Dossovitski A, Missevitch O and Lecoq P
206 2007 *Nucl. Instr. and Meth. A* **571** 122 – 125
207 [4] van Eijk C W E 2002 *Phys. Med. Biol.* **47** R85
208 [5] Levin A and Moisan C 1996 *IEEE Nucl. Sci. Symp. Conference Record.* **2** 702
209 [6] Bellamy E *et al.* 1994 *Nucl. Instr. and Meth. A* **339** 468
210 [7] Liu S 2009 *IEEE Trans. Nucl. Sci.* **56** 2614
211 [8] Bertolaccini M, Cova S and Bussolati C 1968 *Proc. Nucl. Electr. Symp.*
212 [9] Seifert S, van Dam H T and Schaart D R 2012 *Physics in Medicine and Biology* **57** 1797
213 [10] Shao Y 2007 *Phys. Med. Biol.* **52** 1103

Table 1. Properties of the materials used in the simulation.

Material	Chemical composition	Density (g cm ⁻³)	Refractive index
Air	N _{0.76} O _{0.23}	1.29 × 10 ⁻³	1.00
LYSO	Lu ₂ Si ₁ O ₅	7.40	1.82
Meltmount	C ₁ H ₁ O ₁	1.00	1.58
PMTWindow	C ₁ H ₁ O ₁	1.00	1.52
Photocathode	Aluminium	2.70	-

Table 2. Optical Properties of LYSO.

Light yield	Rise time	Decay time	Resolution scale	Bulk light attenuation length
26000 photos/Mev	0.09 ns[9]	40 ns	6.8	40 mm

Table 3. Type and surface finish of each of the optical interfaces defined in the simulations

Name	type	finish	σ_α
LYSO-Frontside	dielectric_dielectric	groundbackpainted	0.1 degrees
LYSO-Foursides	dielectric_dielectric	groundbackpainted	4.0 degrees
LYSO-Meltmount	dielectric_dielectric	ground	0.1 degrees
Meltmount-PMTWindow	dielectric_dielectric	ground	0.1 degrees
PMTWindow-Photocathode	dielectric_metal	ground	0.0 degrees

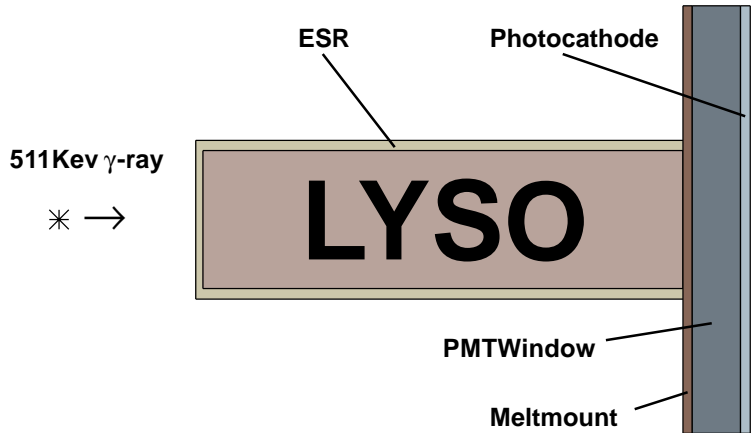


Figure 1. Simplified scheme of the optical volumes and materials used in simulation

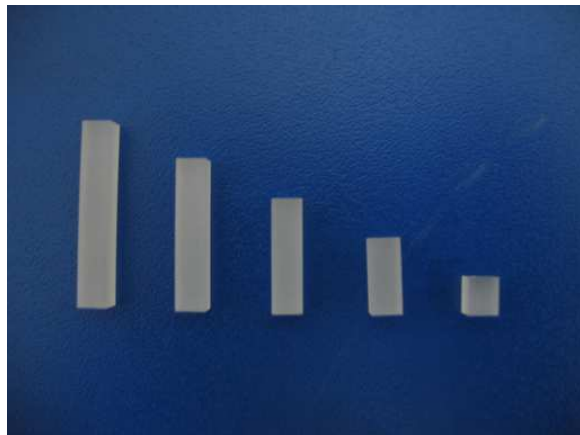


Figure 2. LYSO pixels used in the experiment

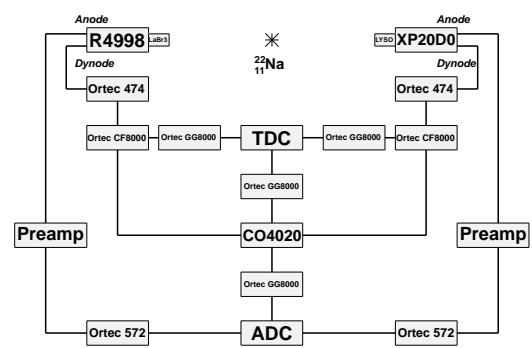


Figure 3. Electronic Configure

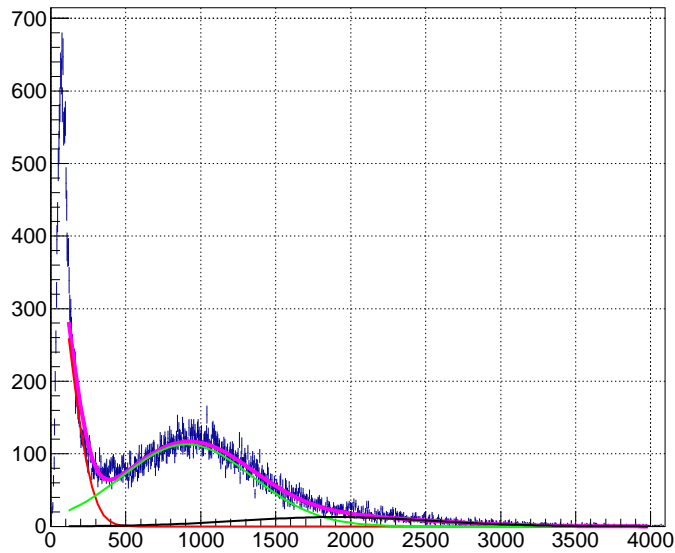


Figure 4. Single Photoelectron Spectrum: magenta line represents the total fit to the spectrum, red line presents gaussian fit to the pedestal, green line represents gaussian fit to the single photo-electron peak and black line represents gaussian fit to the two photo-electrons peak.

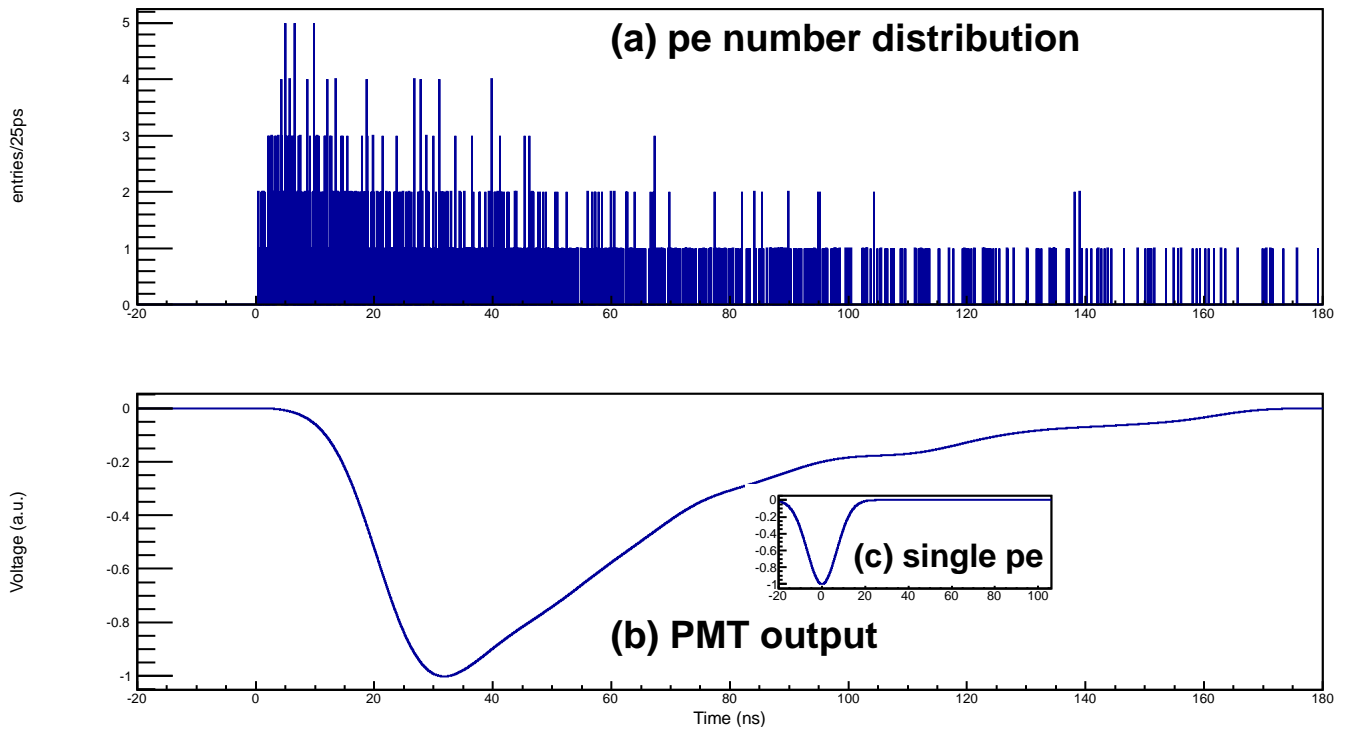
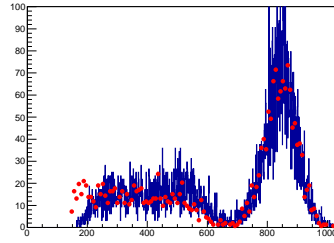
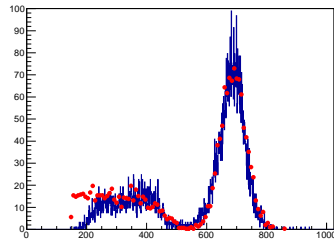


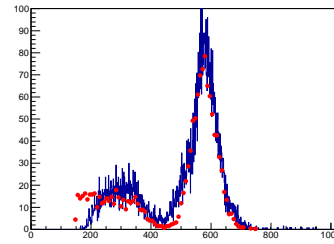
Figure 5. (a) Photoelectrons time distribution on the photocathode, (b) Normalized PMT output signal of a γ -ray event and (c) Normalized PMT response of single photoelectron. Pe = photoelectron.



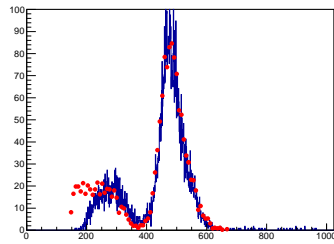
(a)



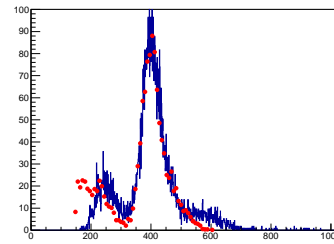
(b)



(c)



(d)



(e)

Figure 6. Experiment (blue line) and simulation (red dot) Energy Spectrum of different LYSO pixel lengths: (a) $L=05$ mm,(b) $L=10$ mm,(c) $L=15$ mm,(d) $L=20$ mm,(e) $L=25$ mm.

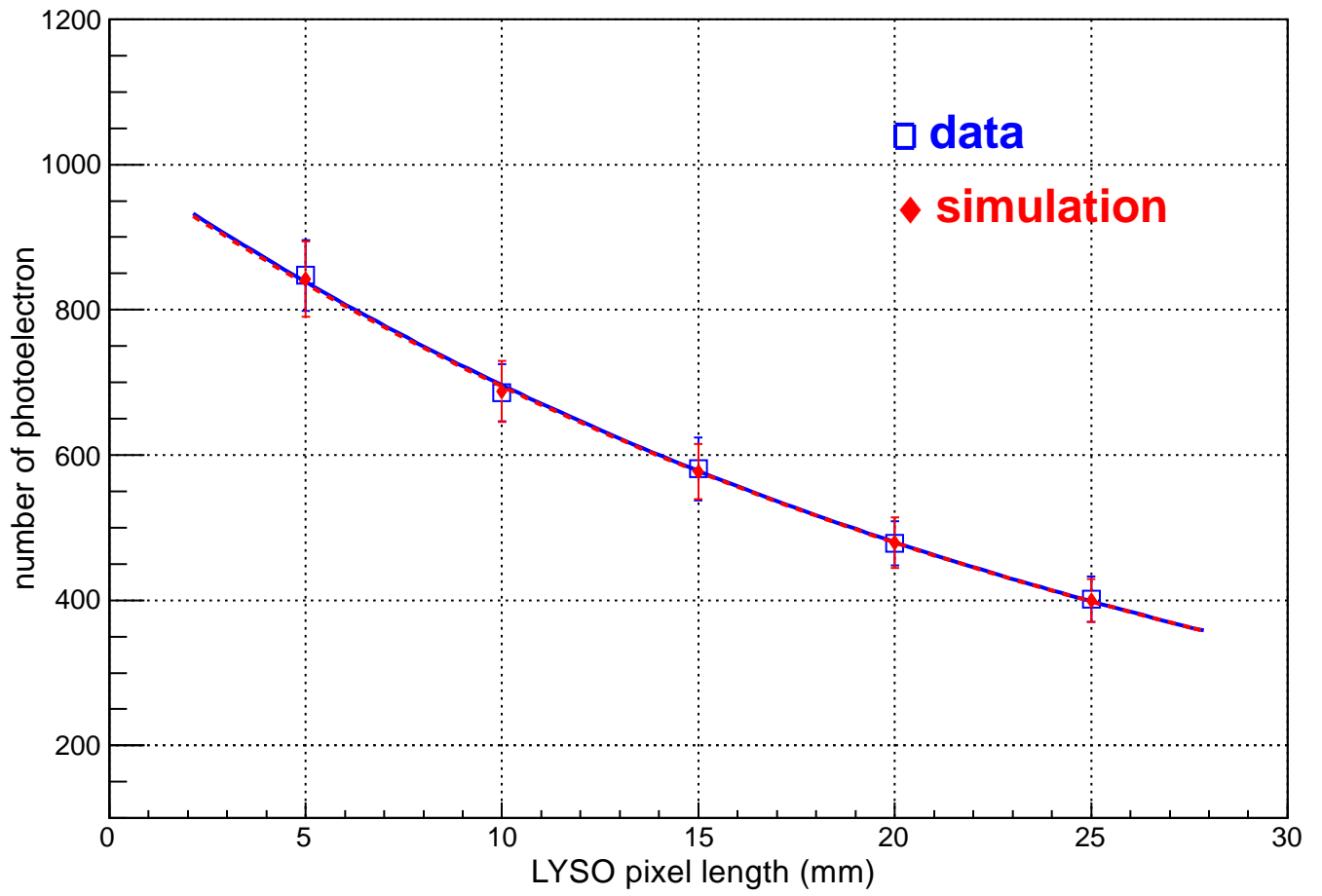


Figure 7. Experiment (box) and simulation (diamond) light yield. Error bars represent one standard deviation of uncertainty.

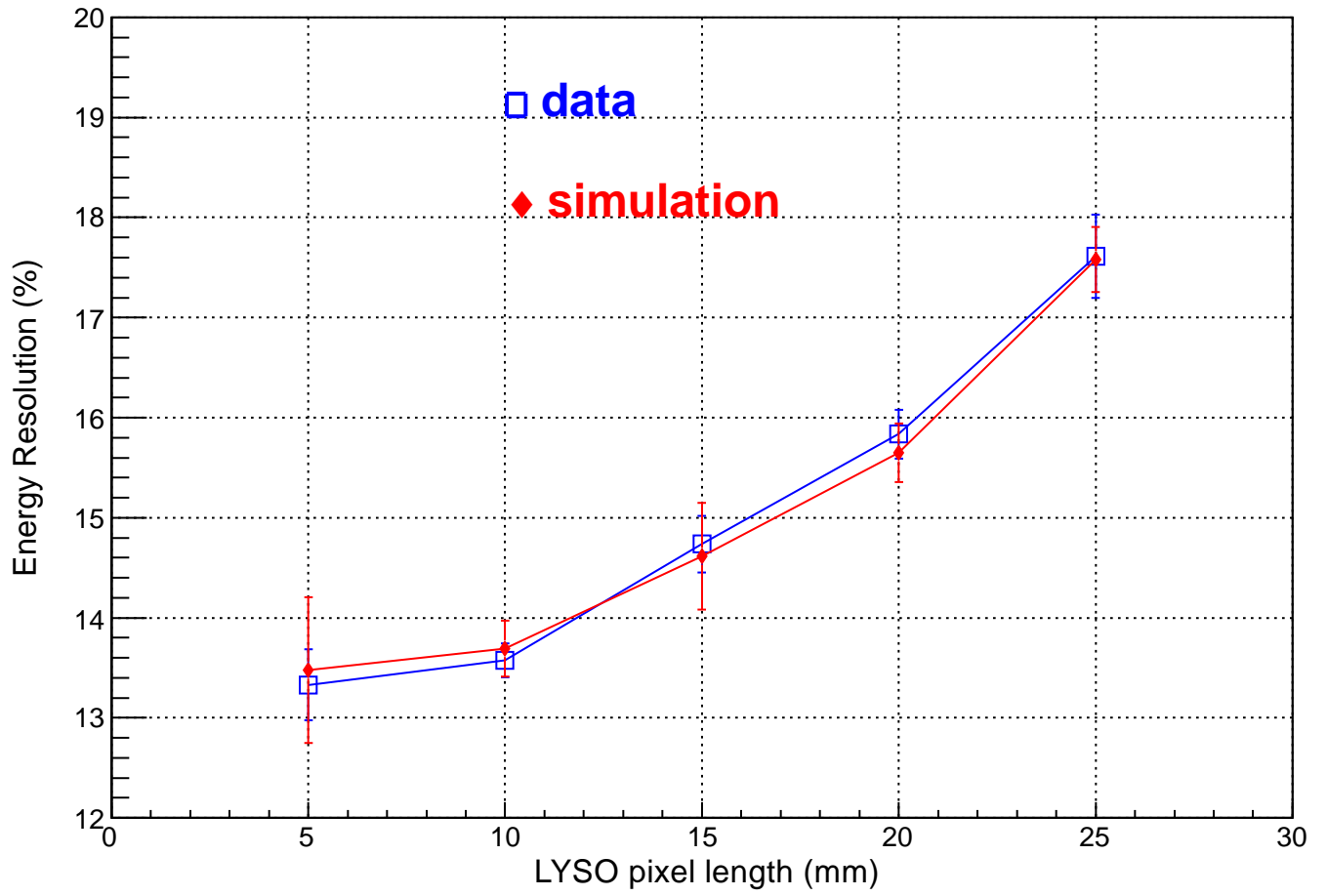


Figure 8. Experiment (box) and simulation (diamond) energy resolution. Error bars represent the statistical errors.

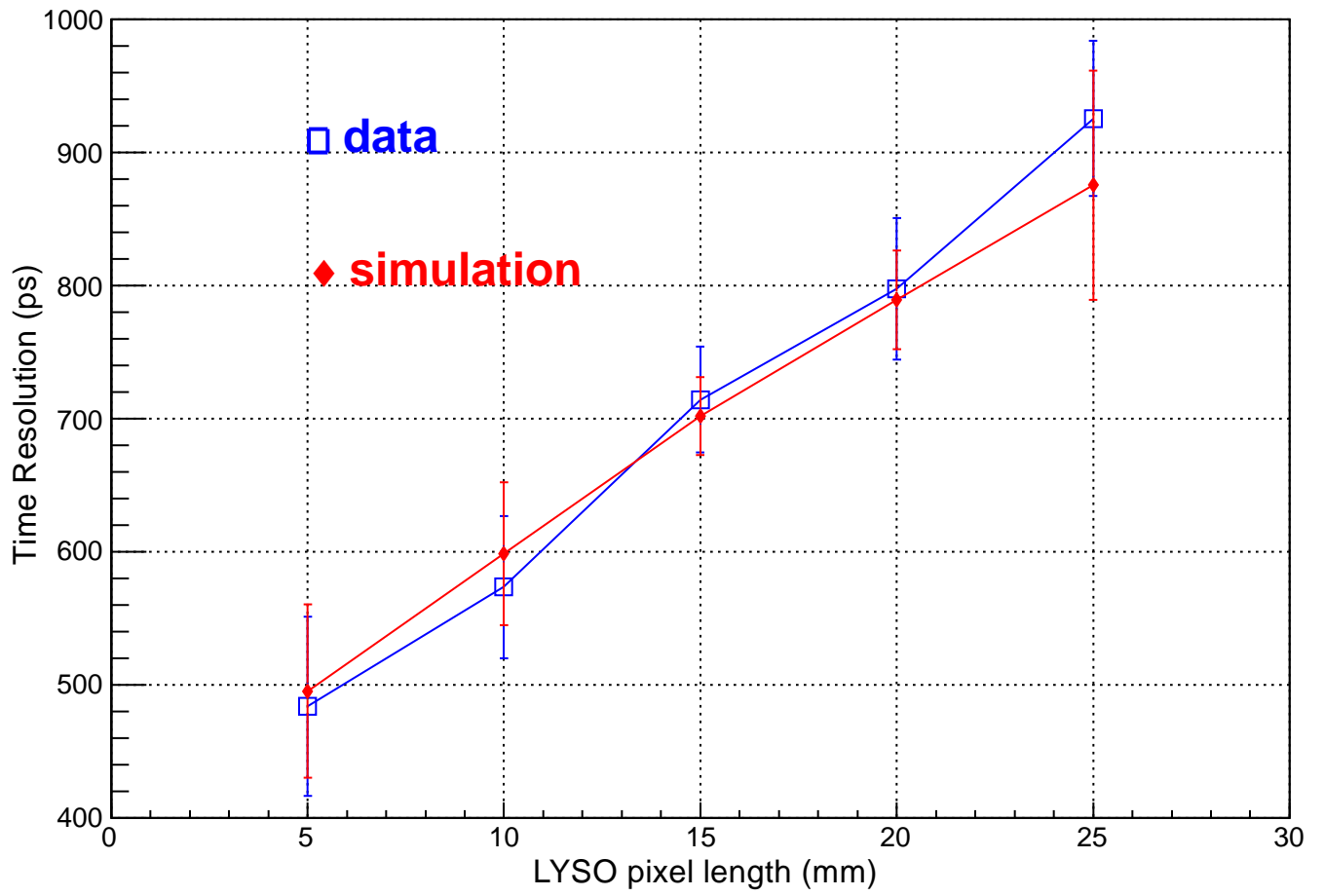


Figure 9. Experiment (box) and simulation (diamond) time resolution. Error bars represent the statistical errors.